QTL mapping of leaf angle on eight nodes in maize enable the optimize canopy by differential operating of leaf angle at different levels of plant

Dengguo Tang[1], Zhengjie Chen[1], Jixing Ni, Qin Jiang, Peng Li, Le Wang, Jinhong Zhou, Chenyang Li and Jian Liu[*]

Maize Research Institute, Sichuan Agricultural University, Huiming Road, Wenjiang District, Chengdu, Sichuan 611000, China; Key Laboratory of Biology and Genetic Improvement of Maize in Southwest Region, Ministry of Agriculture, China

[1]These authors contributed equally to this work

[*]To whom correspondence should be addressed. Tel. +86 28-86290916. Fax +86 28-86290912. E-mail: liujian@sicau.edu.cn

Email addresses of coauthor:

DGT: E-mail: 375339640@qq.com

ZJC: E-mail: 839453983@qq.com

QJ: E-mail: 171491965@qq.com

JXN: E-mail: 345310475@qq.com

PL: E-mail: 1498589736@qq.com

LW: E-mail: 1198253495@qq.com

JHZ: E-mail: 703308243@qq.com

CYL: E-mail: 1575887443@qq.com

The date of submission: 18 December 2018

The number of tables: 5

The number of figures: 1 (colour online-only**)**

The word count: 3,779

The number of supplementary tables: 3

The number of supplementary figure: 1 (colour online-only**)**

QTL mapping of leaf angle on eight nodes in maize enable the optimize canopy by differential operating of leaf angle at different levels of plant

Running title: Regulatory network for leaf angle on eight nodes in maize

Highlight: QTL were identified for maize Leaf angle on different nodes, which has illuminated the genetic control networks of maize LA and empowered canopy ideotype design by manipulate leaf angle at individual leaves.

Abstract

Leaf angle (LA) is one of the most important canopy architecture traits of maize (*Zea mays* L.). To date, there is an urgent need to characterize the genetic control of LA at multiple nodes to bridge the information gap remain in optimizing canopy architecture for maximum yield at different canopy levels. In this study, through the cross between B73 (compact plant architecture) and SICAU1212 (expanded plant architecture), 199 derived RIL families were used to perform QTL mapping for LA from eight leaves at different nodes in three environments, utilizing single-environment analysis and joint mapping. Combining the results of two mapping strategies, we identified 15 common QTL associated with LA at eight nodes. The phenotypic variation explained by the individual QTL ranged from 0.39% to 20.14% and the number of leaves controlled by a single QTL varied from 1 to 8. Among them, QTL *qLA2.1* and *qLA5.1* simultaneously controlled LA of all the eight nodes; however, *qLA2.2* only affected that of 1stLA. The total phenotypic variation explained by all QTL identified for LA at eight nodes ranged from 15.69% (8thLA) to 51.73% (1stLA). The number of QTL detected for LA at each nodes ranged from 4 (7thLA) to 11 (1stLA). These results provide comprehensive insights into the molecular bases of regulatory networks in LA morphogenesis, and will benefit the molecular design breeding of ideotype and further cloning of LA QTL at different plant levels in maize.

Keywords: Leaf angle, eight nodes, canopy architecture, QTL, Regulatory networks, maize

Introduction

Maize (*Zea mays* L.) is one of the most important cereal crops worldwide, and the primary goal of maize breeding programs is to generate high-yielding varieties. During the past several decades, the increase in maize yield was largely due to the increased plant density, rather than improving the potential yield per plant (Duvick, 2005; Ma *et al.*, 2014b; Mock and Pearce, 1975; Russell, 1991; Tollenaar and Wu, 1999). A suite of dramatic changes in plant architecture have been observed, which play a pivotal role in adaptation to high plant density. Some key parameters of optimal plant characteristics were identified as early as in 1970s, including upright leaves, maximum photosynthetic efficiency, and small tassel size and so on (Mock and Pearce, 1975).

Early studies suggested that LA was a critical parameter of plant architecture of impact on light interception and photosynthesis, and plant breeding practices in maize have also shown that LA was an essential agronomic trait in the development and adoption of high-yielding varieties of maize. As breeders focused on improving grain yield, LA score has decreased remarkably, which has mainly shaped plant architecture from expanded to compact plant architecture (Anderson and Denmead, 1969; de Wit, 1965; Duncan *et al.*, 1967; Ku *et al.*, 2010a). Erect canopies can increase in light interception efficiency at higher plant densities, and eventually, leading to increased production. Comprehensive analysis of the correlation between LA trait and grain yield revealed two interesting facts: (1) although the LA had significantly decreased over the past few decades, smaller LA does not guarantee higher yield; and (2) further increase in light interception efficiency needs to vary LA at different parts of maize plant (Duncan, 1971; Lambert and Johnson, 1978; Ma *et al.*, 2014a; Mickelson *et al.*, 2002; Pepper *et al.*, 1977; Winter and Ohlrogge, 1973; Zhang *et al.*, 2017). More recently, Mantilla et al. (2017) has proposed that the optimization of canopy architecture could be manipulated with varying LA at different levels for maximum production potential in cereal species (Mantilla-Perez and Salas Fernandez, 2017).

With the advent of QTL mapping strategies, linkage mapping and association analysis have been conducted in maize to dissect the genetic basis of LA, and hundreds of quantitative trait loci (QTL) for LA have been identified throughout all

ten of the maize chromosomes. Among these studies, there were widely different in number and node position of selected leaves, statistical methods of phenotype data, types of mapping populations and QTL mapping strategies. Detailed information of previous studies showed that research groups chose different number and node positions of leaves for analysis. In most circumstances, three continuous leaves including the ear leaf, the leaves above and below ear were selected for analysis (Ding *et al.*, 2015; Ku *et al.*, 2016; Ku *et al.*, 2012; Ku *et al.*, 2010b; Li *et al.*, 2015; Mickelson *et al.*, 2002; Ming *et al.*, 2007; Shi *et al.*, 2017; Zhang *et al.*, 2017), and in some instances, that of the first leaf below the flag (Pan *et al.*, 2017; Tian *et al.*, 2011; Wang *et al.*, 2017a; Yang *et al.*, 2015b) or two leaves near the ear (Chen *et al.*, 2015; Hou *et al.*, 2015). There were two kinds of statistical methods to phenotype data. QTL mapping was performed using average values for leaves or not/the value of individual leaf. Furthermore, different mapping populations have been adopted, such as $F_{2:3}$ (Chen *et al.*, 2015; Hou *et al.*, 2015; Ku *et al.*, 2012; Ku *et al.*, 2010b; Ming *et al.*, 2007; Yu *et al.*, 2006), F_4 (Chen *et al.*, 2015), RIL (Ku *et al.*, 2016; Li *et al.*, 2015; Mickelson *et al.*, 2002; Shi *et al.*, 2017; Wang *et al.*, 2017a; Yang *et al.*, 2015b; Zhang *et al.*, 2017), Four-Way Cross Mapping Population (Ding *et al.*, 2015), NAM (Tian *et al.*, 2011) and ROAM (Pan *et al.*, 2017). Together with QTL mapping, Tian *et al.* (2011) and Pan *et al.* (2017) identified 203 and 10 single-nucleotide polymorphisms (SNPs) associated with LA through GWAS studies, respectively.

Identification of actual genes responsible for LA QTL and isolation of mutants with altered LA is the critical step to unravel the genetic and molecular mechanisms underlying maize LA. So far, only two LA QTL, *ZmTAC1 (Ku et al., 2011)* and *ZmCLA4 (Zhang et al., 2014)* were identified, and six LA mutants, *liguleless1* (*lg1*) (Moreno *et al.*, 1997), *lg2* (Walsh *et al.*, 1998), *Liguleless3-O* (*Lg3-O*) (Muehlbauer *et al.*, 1999), *Liguleless narrow-Reference* (*Lgn-R*) (Moon *et al.*, 2013), *droopingleaf1* (*drl1*) *and drl2* (Strable *et al.*, 2017) have been cloned. Specifically, *lg1*, *lg2* and *Lgn-R* mutants exhibit a defect in ligule and auricle tissues and a decrease in leaf angle (Harper and Freeling, 1996; Moon *et al.*, 2013; Sylvester *et al.*, 1990; Walsh *et*

115 *al.*, 1998). Notably, *LG1*, *LG2* and *LGN* were shown to act in a common pathway
116 involved in ligule development (Harper and Freeling, 1996; Moon *et al.*, 2013).
117 Similarly, the *Liguleless3-O (Lg3-O)* mutant also develops a decreased leaf angle,
118 which might be due to the defect in transformation of blade-to-sheath at the midrib
119 region in leaf (Fowler *et al.*, 1996; Muehlbauer *et al.*, 1997; Muehlbauer *et al.*, 1999).
120 Nevertheless, the *drl* genes are required for properly development of leaf and leaf
121 support tissues, and for restricting auricle expansion at the midrib, and the LA in the
122 *drl1* and *drl2* mutants are increased (Strable *et al.*, 2017).

123 As mentioned above, only one or a few or average values for leaves were
124 characterized in previous studies, which could not provide valuable information for
125 manipulate LA at canopy level. In the present study, the QTL mapping for LA at eight
126 consecutive leaves were performed with an RIL population, providing valuable
127 information in support of canopy ideotype design and fine mapping of QTL
128 controlling maize LA at different canopy levels.

129 **Materials and Methods**

130 *Mapping populations and Field experiment*

131 The recombinant inbred line population (RIL) was derived from a cross of B73 and
132 SICAU1212, as described previously (Yang *et al.*, 2016; Yang *et al.*, 2015a). The
133 parent B73 with erect leaves is widely used as elite line from the stiff stalk heterotic
134 group and has been partly attributed to the changes in LA of maize varieties since
135 1970, and another parent SICAU1212 with extremely expanded leaves that have been
136 developed from a waxy maize landrace Silunuo by continuously self-pollinating 10
137 times, which was cultivated at least 100 years ago (Tian *et al.*, 2008). 199 of the 325
138 RIL families randomly subsampled from their initial population were used in the
139 present study.

140 The 199 RIL families and their parent lines were grown in a complete
141 randomized block designed with two replications in three distinct environments of
142 China. The three environments locate at Jinghong of Yunnan province (21°57'N,
143 100°45E, elevation 551 m) in 2015 (15JH), Chengdu of Sichuan province (30°43'N,

103°52'E, elevation 500 m) in 2016 (16CD) and Guiyang of Guizhou province (26°29'N, 106°39'E, elevation 1277 m) in 2016 (16GY), respectively. Fourteen plants were cultivated for each single-row plot with a planting density of 52,500 plants ha^{-1} in all environments. Row length was 3.0 m, and row spacing was 67 cm. Field management was the same as the standard cultivation management in accordance with growing season.

Phenotypic measurements and analysis

Five plants from the middle of each plot were used to evaluate the phenotype at 10 d after pollen shed. The leaf angle (LA) of eight consecutive leaves below tassel from each plant was measured as the angle between the vertical line and the base of leaf midrib (Hou *et al.*, 2015). LA of the first leaf was abbreviated to 1stLA, LA of the second leaf below tassel abbreviated to 2ndLA, and so forth. The phenotypic data of LA was determined as the average of each family from two replications in a single environment.

Statistical analysis and Pearson's phenotypic correlations were computed employing IBM SPSS Statistics version 20.0 software (*http://www.spss.com*). Broad-sense heritability (h_B^2) for each LA was estimated as $h_B^2 = \sigma_g^2 / \left(\sigma_g^2 + \sigma_{ge}^2/n + \sigma^2/nr\right)$, where σ_g^2 is the genetic variance, σ_{ge}^2 is the interaction variance between genotype and environment, σ^2 is the error variance, n is the number of environments and r is the number of replications in each environment (Hallauer *et al.*, 2010).

Linkage map and QTL mapping

We re-constructed the linkage map of RIL population that is described in a recent report (Yang *et al.*, 2016). Briefly, the current linkage map was shortened to have 106 SSRs and 154 indels, which spanned 1133.57 cM for the whole genome, and was drawn in the MapChart software version 2.3 (Voorrips, 2002). The QTL for each LA were detected by including composite interval mapping (ICIM) (Li *et al.*, 2008; Li *et al.*, 2007) using the QTL IciMapping software, version 4.0 (*http://www.isbreeding.net/*) in a single-environment. A walking speed of 1.0 cM was selected for QTL mapping,

and the probability in the stepwise regression was set to 0.001. Threshold LOD scores were computed by 1,000 permutations, and a type I error was set at 0.05. The joint mapping, epistatic interaction and QTL by environment interaction (QEI) detection were performed by a mixed-model based composite interval mapping (MCIM) (Wang *et al.*, 1999) using QTLNetwork software version 2.1 (Yang *et al.*, 2008). The testing window size, walk speed and filtration window size of genome scan configuration was set to 10, 1 and 10 cM, respectively. 1,000 permutations at a significance level of $P = 0.05$ was performed to calculate the threshold for declaring the presence of a significant QTL. Positive additive effect indicates that the allele resulting in increased LA is from the compact parent B73, whereas negative effect showing the allele from expanded parent SICAU1212. The QTL for LA of the leaves were considered identical only upon the confidence intervals of QTL were overlapped.. The name of the QTL was assigned as 'q' followed by 'LA', 'maize chromosome on which the corresponding QTL locates', '.', and 'serial number of QTL'. In addition, QTL with PVE (%) > 10% were declared as major QTL. QTL were detected repeatedly in more than one environments were considered as stable QTL

Results

Phenotypic performance of LA from eight consecutive leaves

The phenotypic values of LA were analyzed in RIL families and their parent lines cultivated in three distinct habitats (Table 1). It was obvious that each LA in B73 was significantly different from that in SICAU1212 ($P < 0.01$). All eight leaves tested in the parent line B73 display an almost vertical angle, whereas the other parent line SICAU1212 has more horizontal leaf orientations. In addition, the strong variation extent in all eight LAs can be detected in the RIL lines, although it displays a continuous distribution (Table 1). Specifically, the LA of topper leaves displays a larger variation (around 11-fold) than that of lower leaves (around 3-fold) in the RIL population. In addition, the values of all traits in RIL families exhibited obvious transgressive segregation, indicating that the LA is under polygenic quantitative genetic control.

The estimated broad-sense heritability (h_B^2) for LA in eight leaves ranges from 79.47 to 83.46 % (Table 2), indicating that genetic factors dominantly determine the formation of LA. The lines within the RIL population were significantly ($P < 0.001$) different for all traits (Table 2). Significant ($P < 0.001$) genotype × environment interactions for all traits were also observed. With the exception of 8thLA, the variances of replications for all traits were non-significant ($P < 0.05$). Therefore, the mean of two replications in one environment for each RIL family was used for single-environment mapping. The phenotypic correlation coefficients among distinct LAs within the RIL population are shown in Supplementary Table S1. It revealed that the LA of all leaves has a significantly positive correlation ($P < 0.001$) (Supplementary Table S1). Moreover, the LA of more adjacent leaves displays a much higher correlation coefficients (Supplementary Table S1).

QTL analysis

Using inclusive composite interval mapping, a total of 56 putative QTL for LA at eight nodes were identified, and 11 QTL were common between leaves or environments (Supplementary Table S2, Supplementary Fig.S1). Of these 11 common QTL, three QTL were identified on chromosome 5, two QTL on chromosome 3 and one QTL on chromosome 1, 2, 4, 6, 8 and 9. Five QTLs were detected in more than one environment. With the exception of *qLA6.1* controlling 1stLA, all QTL had the negative additive effect in the single-environment analysis. The individual effect of QTL ranged from 5.62% to 20.14% and the number of leaves controlled by a single QTL varied from 1 to 8. The number of QTL detected for LA at each node ranged from 3 (8thLA) to 8 (1stLA). The total phenotypic variation explained by all QTL identified for LA at eight nodes ranged from 15.69% (8thLA) to 51.73% (1stLA).

Meanwhile, forty-four significant QTL for LA at eight nodes were detected in joint analysis, and 12 QTL were common between leaves (Supplementary Table S3, Supplementary Fig.S1). Of these 12 common QTL, eight were identical to those of the QTL identified by single-environment QTL analysis. The other 4 QTL were specific for the joint mapping, which are QTL *qLA2.2* on chromosome 2, *qLA4.2* on

chromosome 4, *qLA5.4* on chromosome 5 and *qLA7.1* on chromosome 7. These QTL controlled one, five, one and four nodes, respectively; and accounted for 2.11%, 2.306%, 1.29% and 2.34% of phenotypic variance, respectively.

All QTL except *qLA2.2* and *qLA4.2* had a negative additive effect. Together, the results suggested that most of the alleles with a contribution on increasing LA are segregated from SICAU1212 with expanded plant architecture. Notably, Several alleles associated with increased LA were contributed by SICAU1212.

QEIs

Four QTL were involved in significant QTL × environment interaction (QEI) (Table 4) through joint analysis. Three of them are common QTL (*qLA5.3*), which affected the LA of the 2nd, 3rd and 7th leaves simultaneously, and the additive × environment interactions for LA were responsible for 1.89-2.46 % of phenotypic variation. The other QTL (*qLA5.2*) association with the LA of 6^{th} leaf, and the effect of additive × environment interaction was 1.50 %.

Epistatic interaction

A total of twenty ($P < 0.05$) epistatic interactions with additive-by-additive effects were identified for eight LAs, and individual variance ranged from 0.39 to 3.54% (Table 5). Three types of epistatic interactions were identified, including interactions occurred within the genetic region of the QTL identified, between significant QTL and non-significant QTL region, and in non-significant QTL regions. Moreover, the number of LA that individual epistatic interaction affected varied, ranging from 1 to 4. For example, the interaction between *qLA5.3* and *qLA7.1* affected 1stLA to 4thLA, the interaction between marker intervals of chr9-90756–mmc0051 and chr10-77445–umc1336 affected just 2ndLA. On the other hand , the interactions identified for the eight LAs also varied, ranged from 0 to 6. For example, five epistatic interactions were identified for 2ndLA, while no epistatic interaction was identified for 8thLA. In addition, the interaction between epistasis and the environment was not detected in this study.

Discussion

LA exhibits extensive phenotypic variation in single maize plant and population

Both allelic LA in maize population and LA between nodes of a single plant exhibits extensive phenotypic variation. For LA in maize population, among plant architecture-related traits, LA was the second highest degree of variation traits, which second only to tassel branch number (Pan *et al.*, 2017). Early evidence suggested that the upper LA of 26 parental lines for maize NAM population ranged from approximately 30° to 80° (Tian *et al.*, 2011). Likewise, in a recent study, the range of allelic LA in ten maize elite inbred lines was up to four fold (Pan *et al.*, 2017). Additionally, the allelic LA of our mapping population displayed larger variation, ranging from 3-fold (1stLA in 2015JH) to 11-fold (8thLA in 2016CD) change. It's worth mentioning that transgressive phenotypes were observed in various segregating populations.

Phenotypic variation is the variability in phenotypes that exists at different nodes in a single maize plant. Taking a high-yielding maize hybrid (Pioneer 335) as an example, the average LA of three leaves above ear, three ear leaves and three leaves below ear were 22.9°, 32.8° and 41.9°, respectively, and there was ~2.0-fold change between uppermost and lower LA (Ma *et al.*, 2014b). In present study, approximately 1.6-fold difference was observed among the eight LAs of SICAU1212 parental inbred lines, while approximately 2.6-fold that of B73 (Supplementary Table S1). In summary, these results suggest that diversified genetic mechanisms were responsible for LA morphogenesis of a single plant and population.

QTL hotspot regions and pleiotropic QTL response for morphogenesis of LA

Hundreds of QTL or SNPs associated with LA were identified from various genetic backgrounds, which provided valuable genetic information. However, the difference between research methods led to problems in comparative analysis, particularly node position of selected leaves. For example, ear position of maize was frequently used as a reference position to selection leaves for LA analysis. Nevertheless, the study of the leaves of the relative positions to ear leaf is not conducive to the comparative analysis

of the results. In spite of that, distribution characteristics of QTL controlling LA trait still could be seen to a certain degree by comparative analysis. In present study, fifteen QTL controlled LAs of eight consecutive leaves were detected, which was highly consistent with the results of previous studies. Moreover, these QTL were not randomly distributed on whole genome, but were located on a few genomic regions. There were eight hotspot regions for LA, which are distributed on chromosomes 1, 2, 4, 5, 8 and 9. Of these QTL, the number of times detected by sixteen different LA studies ranged from 5 to 11 (Table 3). Among them, *qLA2.1*, located on short arm of chromosome 2, were detected in most previous studies (Ding *et al.*, 2015; Hou *et al.*, 2015; Ku *et al.*, 2012; Mickelson *et al.*, 2002; Ming *et al.*, 2007; Pan *et al.*, 2017; Shi *et al.*, 2017; Tian *et al.*, 2011; Wang *et al.*, 2017b; Yang *et al.*, 2015b; Zhang *et al.*, 2017). In addition, the hotspot QTL *qLA1.1*, harbors the cloned LA mutant gene, *drooping leaf1* (*drl1*) (Strable *et al.*, 2017); *qLA2.1* contains *liguleless1* (*lg1*) (Becraft *et al.*, 1990; Becraft and Freeling, 1991; Moreno *et al.*, 1997; Sylvester *et al.*, 1990).

Pleiotropic QTL played an important role of LA at different nodes, and tended to control the consecutive LAs. Of fifteen identified QTL in this study, approximately seventy percent QTL controlled more than two LAs. The frequency of QTL that were identified in different genetic backgrounds was positively correlated with number of LA on different nodes that were controlled by QTL. More interestingly, the distribution of these LAs controlled by pleiotropic QTL exhibited spatial-specificity. Some QTL controlled all eight LAs, some QTL controlled LA of upper layers, and some QTL controlled LA of lower layers. For example, *qLA3.1* affected LA of upper layers, 1stLA to 4thLA, while *qLA9.1* controlled LA of lower layers, 5thLA to 8thLA. It is worth noting that the fine mapping of pleiotropic QTL can be carried out for a specific leaf controlled by the QTL with stable and major effects.

The genetic architecture of the eight leaf angles exhibits extensive diversity

Not only the result of present study, but also that of most previous studies (Ding *et al.*, 2015; Hou *et al.*, 2015; Ku *et al.*, 2010b; Pan *et al.*, 2017; Shi *et al.*, 2017; Tian *et al.*, 2011; Wang *et al.*, 2017b; Yang *et al.*, 2015b) demonstrated that genetic factors were a

major determinant of LA traits and the heritability of LA trait estimates were largely similar between adjacent nodes. More interestingly, QTL analysis for LA at eight nodes had indicated that there were different sets of QTL that controlled LA at different nodes. The result revealed a rich genetic architecture of LA trait: (ⅰ) The results showed that the LA trait was controlled by major gene plus polygenes genetic model with difference in detail. The number and effects size of major QTL were not the same for different nodes, and the number of major QTL ranged 1 (8thLA) to 4 (1stLA), and the highest PVE value was 20.14%. Additionally, the major QTL had been identified in most QTL mapping studies of LA in maize (Chen *et al.*, 2015; Ku *et al.*, 2010b; Pan *et al.*, 2017), however, a few studies fail to find major QTL (Hou *et al.*, 2015; Tian *et al.*, 2011). (ⅱ) The epistatic interaction identified for LA of different leaf nodes showed that there were difference in absence or presence with the different number of loci. No epistatic interactions were observed for the 8thLA, while epistatic interaction was identified for others, ranging from 1 (5thLA) to 5 (2ndLA). (ⅲ) the LA at different nodes have different QTL × environment interaction (QEI). Four LA, including 2ndLA, 3rdLA, 6thLA: QEI of *qLA5.2* and 7thLA, were affected by QEI at different levels. The rest LA had not detected QEI. Taking together, the data indicated that the genetic architecture underlying the eight LAs exhibits extensive diversity.

Application for canopy ideotype breeding by design at different canopy levels design in maize

The result of this research bridges the crucial knowledge gap between theory and breeding practice. For instance, node-specificity QTL could be applied directly to the manipulation of the leaf angle, and region-specificity QTL could shape the LA of upper, middle or lower canopy, separately, and environment-specificity QTL could be used in ecological idotype breeding. Additionally, other controls of leaf angle operate could been employed by combined use of the pleiotropic QTL, based on different effect size of QTL. It is however worth mentioning that this study not only provides the theoretical basis of regulatory network for designing LA differently but also

unlock the door for further dissecting the LA trait in cereal crop.

Furthermore, QTL mapping of LA at multiple levels, together with our previous research of QTL controlled leaf wide on eight nodes, provides a comprehensive strategy for maize "smart canopy" breeding, which was proposed by Ort et al. (2015) for improving canopy architecture and metabolic features of leaves interacting cooperatively throughout the canopy to maximize yield potential (Ort *et al.*, 2015; Yang *et al.*, 2016).

Supplementary data

Table S1. Phenotypic correlation coefficients between eight LAs across three environments

Table S2. Putative QTL for LA in the RIL population through single-environment QTL mapping

Table S3. QTL for eight LAs detected in joint analysis across three environments

Fig S1. Genetic linkage map of the RILs and locations of QTLs for eight LAs in single-environment QTL mapping and joint analysis

Acknowledgements

The authors are grateful to the National Basic Research Program of China (the "973" project, Grant No. 2014CB138203), the State Key Laboratory of Grassland Agro-ecosytems, China (SKLGAE201509) and the National Natural Science Foundation of China (31101161).

Reference

Anderson MC, Denmead O. 1969. Short wave radiation on inclined surfaces in model plant communities. *Agronomy Journal* **61**, 867-872.

Becraft PW, Bongard-Pierce DK, Sylvester AW, Poethig RS, Freeling M. 1990. The liguleless-1 gene acts tissue specifically in maize leaf development. *Developmental biology* **141**, 220-232.

Becraft PW, Freeling M. 1991. Sectors of liguleless-1 tissue interrupt an inductive signal during maize leaf development. *Plant Cell* **3**, 801-807.

Chen X, Xu D, Liu Z, Yu T, Mei X, Cai Y. 2015. Identification of QTL for leaf angle and leaf space above ear position across different environments and generations in maize (Zea mays L.). *Euphytica* **204**, 395-405.

de Wit CT. 1965. Photosynthesis of leaf canopies. Pudoc.

Ding J, Zhang L, Chen J, Li X, Li Y, Cheng H, Huang R, Zhou B, Li Z, Wang J, Wu J. 2015. Genomic Dissection of Leaf Angle in Maize (Zea mays L.) Using a Four-Way Cross Mapping Population. *PloS one* **10**, e0141619.

Duncan W. 1971. Leaf angles, leaf area, and canopy photosynthesis. *Crop Science* **11**, 482-485.

Duncan W, Loomis R, Williams W, Hanau R. 1967. A model for simulating photosynthesis in plant communities. *California Agriculture* **38**, 181-205.

Duvick DN. 2005. The Contribution of Breeding to Yield Advances in maize (Zea mays L.). **86**, 83-145.

Fowler JE, Muehlbauer GJ, Freeling M. 1996. Mosaic analysis of the liguleless3 mutant phenotype in maize by coordinate suppression of mutator-insertion alleles. *Genetics* **143**, 489-503.

Hallauer AR, Carena MJ, Miranda Filho Jd. 2010. *Quantitative genetics in maize breeding*: Springer Science & Business Media.

Harper L, Freeling M. 1996. Interactions of liguleless1 and liguleless2 function during ligule induction in maize. *Genetics* **144**, 1871-1882.

Hou X, Liu Y, Xiao Q, Wei B, Zhang X, Gu Y, Wang Y, Chen J, Hu Y, Liu H,

Zhang J, Huang Y. 2015. Genetic analysis for canopy architecture in an F2:3 population derived from two-type foundation parents across multi-environments. *Euphytica* **205**, 421-440.

Ku L, Ren Z, Chen X, Shi Y, Qi J, Su H, Wang Z, Li G, Wang X, Zhu Y, Zhou J, Zhang X, Chen Y. 2016. Genetic analysis of leaf morphology underlying the plant density response by QTL mapping in maize (Zea mays L.). *Molecular Breeding* **36**.

Ku L, Wei X, Zhang S, Zhang J, Guo S, Chen Y. 2011. Cloning and characterization of a putative TAC1 ortholog associated with leaf angle in maize (Zea mays L.). *PloS one* **6**, e20621.

Ku L, Zhao W, Zhang J, Wu L, Wang C, Wang P, Zhang W, Chen Y. 2010a. Quantitative trait loci mapping of leaf angle and leaf orientation value in maize (Zea mays L.). *Theoretical and applied genetics* **121**, 951-959.

Ku LX, Zhang J, Guo SL, Liu HY, Zhao RF, Chen YH. 2012. Integrated multiple population analysis of leaf architecture traits in maize (Zea mays L.). *J Exp Bot* **63**, 261-274.

Ku LX, Zhao WM, Zhang J, Wu LC, Wang CL, Wang PA, Zhang WQ, Chen YH. 2010b. Quantitative trait loci mapping of leaf angle and leaf orientation value in maize (Zea mays L.). *Theor Appl Genet* **121**, 951-959.

Lambert R, Johnson R. 1978. Leaf Angle, Tassel Morphology, and the Performance of Maize Hybrids 1. *Crop Science* **18**, 499-502.

Li C, Li Y, Shi Y, Song Y, Zhang D, Buckler ES, Zhang Z, Wang T, Li Y. 2015. Genetic control of the leaf angle and leaf orientation value as revealed by ultra-high density maps in three connected maize populations. *PloS one* **10**, e0121624.

Li H, Ribaut JM, Li Z, Wang J. 2008. Inclusive composite interval mapping (ICIM) for digenic epistasis of quantitative traits in biparental populations. *Theor Appl Genet* **116**, 243-260.

Li H, Ye G, Wang J. 2007. A modified algorithm for the improvement of composite interval mapping. *Genetics* **175**, 361-374.

Ma D-L, Xie R-Z, Niu X-K, Li S-K, Long H-L, Liu Y-E. 2014a. Changes in the

morphological traits of maize genotypes in China between the 1950s and 2000s. *European journal of agronomy* **58**, 1-10.

Ma DL, Xie RZ, Niu XK, Li SK, Long HL, Liu YE. 2014b. Changes in the morphological traits of maize genotypes in China between the 1950s and 2000s. *European Journal of Agronomy* **58**, 1-10.

Mantilla-Perez MB, Salas Fernandez MG. 2017. Differential manipulation of leaf angle throughout the canopy: current status and prospects. *Journal of Experimental Botany*.

Mickelson S, Stuber C, Senior L, Kaeppler S. 2002. Quantitative trait loci controlling leaf and tassel traits in a B73× Mo17 population of maize. *Crop science* **42**, 1902-1909.

Ming L, Fang Z, Chuan-Xiao X, Ming-Shun L, Xu Y, Warburton M, Shi-Huang Z. 2007. Construction of a SSR linkage map and mapping of quantitative trait loci (QTL) for leaf angle and leaf orientation with an elite maize hybrid.

Mock J, Pearce R. 1975. An ideotype of maize. *Euphytica* **24**, 613-623.

Moon J, Candela H, Hake S. 2013. The Liguleless narrow mutation affects proximal-distal signaling and leaf growth. *Development* **140**, 405-412.

Moreno MA, Harper LC, Krueger RW, Dellaporta SL, Freeling M. 1997. liguleless1 encodes a nuclear-localized protein required for induction of ligules and auricles during maize leaf organogenesis. *Genes & Development* **11**, 616-628.

Muehlbauer GJ, Fowler JE, Freeling M. 1997. Sectors expressing the homeobox gene liguleless3 implicate a time-dependent mechanism for cell fate acquisition along the proximal-distal axis of the maize leaf. *Development* **124**, 5097-5106.

Muehlbauer GJ, Fowler JE, Girard L, Tyers R, Harper L, Freeling M. 1999. Ectopic Expression of the Maize Homeobox GeneLiguleless3 Alters Cell Fates in the Leaf. *Plant Physiol* **119**, 651-662.

Ort DR, Merchant SS, Alric J, Barkan A, Blankenship RE, Bock R, Croce R, Hanson MR, Hibberd JM, Long SP. 2015. Redesigning photosynthesis to sustainably meet global food and bioenergy demand. *Proceedings of the national*

academy of sciences **112**, 8529-8536.

Pan Q, Xu Y, Li K, Peng Y, Zhan W, Li W, Li L, Yan J. 2017. The genetic basis of plant architecture in 10 maize recombinant inbred line populations. *Plant Physiol*.

Pepper G, Pearce R, Mock J. 1977. Leaf orientation and yield of maize. *Crop science* **17**, 883-886.

Russell WA. 1991. Genetic Improvement of Maize Yields. **46**, 245-298.

Shi Y, Wang X, Guo S, Ren Z, Ku L, Zhu Y, Li G, Qi J, Zhang X, Ren Z, Chen Y, Lübberstedt T. 2017. Detection of epistatic and environmental interaction QTLs for leaf orientation-related traits in maize. *Plant Breeding* **136**, 33-40.

Strable J, Wallace JG, Unger-Wallace E, Briggs S, Bradbury P, Buckler ES, Vollbrecht E. 2017. Maize YABBY Genes drooping leaf1 and drooping leaf2 Regulate Plant Architecture. *Plant Cell*.

Sylvester AW, Cande WZ, Freeling M. 1990. Division and differentiation during normal and liguleless-1 maize leaf development. *Development* **110**, 985-1000.

Tian F, Bradbury PJ, Brown PJ, Hung H, Sun Q, Flint-Garcia S, Rocheford TR, McMullen MD, Holland JB, Buckler ES. 2011. Genome-wide association study of leaf architecture in the maize nested association mapping population. *Nat Genet* **43**, 159-162.

Tian M, Tan G, Liu Y, Rong T, Huang Y. 2008. Origin and evolution of Chinese waxy maize: evidence from the Globulin-1 gene. *Genetic Resources and Crop Evolution* **56**, 247-255.

Tollenaar M, Wu J. 1999. Yield Improvement in Temperate Maize is Attributable to Greater Stress Tolerance. *Crop science* **39**, 1597.

Voorrips R. 2002. MapChart: software for the graphical presentation of linkage maps and QTLs. *Journal of heredity* **93**, 77-78.

Walsh J, Waters CA, Freeling M. 1998. The maize geneliguleless2 encodes a basic leucine zipper protein involved in the establishment of the leaf blade–sheath boundary. *Genes & Development* **12**, 208-218.

Wang D, Zhu J, Li Z, Paterson A. 1999. Mapping QTLs with epistatic effects and

QTL× environment interactions by mixed linear model approaches. *TAG Theoretical and Applied Genetics* **99**, 1255-1264.

Wang H, Liang Q, Li K, Hu X, Wu Y, Wang H, Liu Z, Huang C. 2017a. QTL analysis of ear leaf traits in maize (Zea mays L.) under different planting densities. *The Crop Journal*.

Wang H, Liang Q, Li K, Hu X, Wu Y, Wang H, Liu Z, Huang C. 2017b. QTL analysis of ear leaf traits in maize (Zea mays L.) under different planting densities. *The Crop Journal*.

Winter SR, Ohlrogge AJ. 1973. Leaf Angle, Leaf Area, and Corn (Zea mays L.) Yield. *Agronomy Journal* **65**, 395-397.

Yang C, Tang D, Qu J, Zhang L, Zhang L, Chen Z, Liu J. 2016. Genetic mapping of QTL for the sizes of eight consecutive leaves below the tassel in maize (Zea mays L.). *Theor Appl Genet* **129**, 2191-2209.

Yang C, Tang D, Zhang L, Liu J, Rong T. 2015a. Identification of QTL for ear row number and two-ranked versus many-ranked ear in maize across four environments. *Euphytica* **206**, 33-47.

Yang GH, Dong YB, Li YL, Wang QL, Shi QL, Zhou Q. 2015b. Integrative detection and verification of QTL for plant traits in two connected RIL populations of high-oil maize. *Euphytica* **206**, 203-223.

Yang J, Hu C, Hu H, Yu R, Xia Z, Ye X, Zhu J. 2008. QTLNetwork: mapping and visualizing genetic architecture of complex traits in experimental populations. *Bioinformatics* **24**, 721-723.

Yu Y, Zhang J, Shi Y, Song Y, Wang T, Li Y. 2006. QTL analysis for plant height and leaf angle by using different populations of maize. *J Maize Sci* **14**, 88-92.

Zhang J, Ku L, Han Z, Guo S, Liu H, Zhang Z, Cao L, Cui X, Chen Y. 2014. The ZmCLA4 gene in the qLA4-1 QTL controls leaf angle in maize (Zea mays L.). *J Exp Bot* **65**, 5063-5076.

Zhang X, Huang C, Wu D, Qiao F, Li W, Duan L, Wang K, Xiao Y, Chen G, Liu Q, Xiong L, Yang W, Yan J. 2017. High-Throughput Phenotyping and QTL Mapping

Reveals the Genetic Architecture of Maize Plant Growth. *Plant Physiol* **173**, 1554-1564.

Table 1. Phenotypic performance for leaf angle of RIL population and parents under three environments

Trait	15JH					16CD					16GY[b]				
	B73	SICAU1212	RIL			B73	SICAU1212	RIL			B73	SICAU1212	RIL		
			Mean	SD	Range			Mean	SD	Range			Mean	SD	Range
1stLA	15.11	87.77**	41.80	17.46	10.95-122.05	13.27	69.65**	33.18	14.63	13.72-105.15	20.04	71.39**	41.13	15.95	16.17-87.64
2ndLA	11.63	84.58**	34.57	13.08	11.35-86.85	14.53	48.97**	27.35	9.62	12.48-68.24	21.26	62.23**	38.26	13.036	17.40-86.73
3rdLA	15.78	80.52**	33.68	12.21	14.05-78.44	16.49	43.82**	26.83	9.13	12.92-63.64	24.78	52.47**	38.15	12.18	18.41-82.90
4thLA	18.33	69.02**	34.64	11.97	13.66-103.63	18.50	46.95**	27.67	9.53	12.26-67.42	28.05	51.76**	38.55	11.49	18.22-81.88
5thLA	23.78	60.84**	37.54	10.58	13.41-83.10	20.54	50.86**	31.02	9.92	12.44-78.84	29.66	55.72**	40.77	12.05	19.48-83.71
6thLA	29.41	58.12**	40.82	9.65	16.07-83.97	27.43	59.25**	35.29	9.75	15.62-77.34	34.70	63.25**	44.32	13.29	24.00-83.81
7thLA	34.00	49.33**	40.02	8.36	17.29-69.70	34.87	60.82**	37.46	8.76	16.50-67.52	38.8	67.29**	45.04	12.38	23.08-88.90
8thLA	30.93	46.31**	39.20	8.04	19.49-73.40	37.56	59.77**	38.22	8.31	21.42-66.96	42.42	64.52**	44.93	12.60	21.27-81.90

15JH, 16CD and 16GY represent Jinghong of Yunnan province in 2015, Chengdu of Sichuan province and Guiyang of Guizhou province in 2016, respectively, respectively

** indicates significant level at $P < 0.01$

Table 2. Analysis of variance (ANOVA) for LA for the RIL population in three environments

Source of variation	Mean square							
	1stLA	2ndLA	3rdLA	4thLA	5thLA	6thLA	7thLA	8thLA
Environment (E)	9966.08***	12394.80***	13288.85***	12193.37***	9536.30***	7790.14***	6213.45***	6187.40***
Genotype (G)	705.19***	357.06***	292.89***	291.92***	267.25***	269.66***	238.37***	240.52***
G × E	349.42***	197.47***	180.40***	198.24***	168.31***	181.75***	170.71***	163.32***
Replication	2.76	23.50	180.95	79.70	29.56	129.28	3.47	180.63*
Error	139.70	64.72	62.40	55.98	52.13	50.75	46.40	39.71
h_B^2	83.46	82.33	80.59	79.47	80.49	79.62	78.67	79.75

h_B^2 the broad-sense heritability

*, ** and *** indicate significant level at $P < 0.05$, $P < 0.01$ and $P < 0.001$, respectively

Table 3. Main features of the QTL for eight LAs based on single-environment QTL mapping and joint analysis across three environments

QTL	Bin	1stLA[a]	2ndLA	3rdLA	4tYLA	5tYLA	6tYLA	7tYLA	8tYLA	References[b]
qLA1.1	1.02-1.03	Y	-	Y	-	-	Y	-	-	1,2,3,4,5,6,10,11,12,13,15
qLA2.1	2.01-2.02	Y;**J**	Y,S;**J**	Y;**J**	Y;**J**	Y;**J**	**J**	Y,S;**J**	Y	2,3,5,7,8,9,10,12,13,14,16
qLA2.2	2.07	**J**	-	-	-	-	-	-	-	6,12,14
qLA3.1	3.06	Y;**J**	Y,S,G;**J**	Y;**J**	Y,S	-	-	-	-	9,12
qLA3.2	3.06-3.07	G	-	G	G;**J**	G;**J**	**J**	-	-	12
qLA4.1	4.05	-	-	-	-	-	Y	-	-	12,14
qLA4.2	4.09	-	**J**	**J**	-	**J**	**J**	-	**J**	3,10,12,14,15
qLA5.1	5.03	Y,S;**J**	Y,S,G;**J**	Y,S,G;**J**	S,G;**J**	Y,S,G;**J**	S;**J**	Y,S,G;**J**	S,G;**J**	8,10,12,13,16
qLA5.2	5.04	-	-	-	**J**	-	G;**J**	-	-	1,2,3,5,6,12
qLA5.3	5.06-5.07	G;**J**	G;**J**	G;**J**	G;**J**	-	**J**	G;**J**	-	3,8,9,10,12
qLA5.4	5.07-5.08	-	-	-	-	**J**	-	-	-	3,10,12
qLA6.1	6.01	Y	-	-	-	-	-	-	-	8,12
qLA7.1	7.01-7.02	**J**	**J**	**J**	**J**	-	-	-	-	2,12,14
qLA8.1	8.06-8.07	S;**J**	-	-	-	-	-	-	-	2,7,8,10,11,12,14,16
qLA9.1	9.04	-	-	-	-	S;**J**	S;**J**	S	Y,S;**J**	3,7,10,12,14

[a] The capital letters Y, S and G represent QTL detected at Jinghong of Yunnan province in 2015, Chengdu of Sichuan province and Guiyang of Guizhou province in 2016, respectively. **J** represents QTL detected by joint analysis across three environments.

[b] The number 1 represents Chen et al. 2015, and 2 represents Ding et al. 2015, and 3 represents Hou et al. 2015, and 4 represents Ku et al. 2016, and 5 represents Ku et al. 2012, and 6 represents Ku et al. 2010, and 7 represents Li et al. 2015, and 8 represents Mickelson et al. 2002, and 9 represents Ming et al. 2007, and 10 represents Pan et al. 2017, and 11 represents Shi et al. 2017, and 12 represents Tian et al. 2011, and 13 represents Wang et al. 2017, and 14 represents Yang et al. 2015b, and 15 represents Yu et al. 2006, and 16 represents Zhang et al. 2017.

Table 4. QTLs × Environment (QE) interactions effects for LA identified in the RIL population using QTLNetwork

Traits	QTL	Marker interval	AE1(15JH)	AE2(16CD)	AE3(16GY)	H^2(ae)(%)
2ndLA	*qLA5.3*	chr5-199388–umc2198		1.90*	-2.79**	2.05
3rdLA	*qLA5.3*	chr5-199388–umc2198		1.92**	-2.32**	1.89
6thLA	*qLA5.2*	chr5-139354–chr5-160457			-1.29*	1.50
7thLA	*qLA5.3*	chr5-199388–umc2198			-2.07**	2.46

AE is the additive by designated environment interaction effect

H^2(ae)(%) is contribution rate of additive by environment interaction

*, ** and *** indicate significant level at $P < 0.05$, $P < 0.01$ and $P < 0.001$, respectively

Table 5. Digenetic epistatic QTL for LA identified in the RIL population across three environments

Trait	QTL_i/Marker interval_i	range_i (cM)	QTL_j/Marker interval_j	range_j (cM)	AA	H^2(aa)(%)
1stLA	*qLA3.1*	55.2-59.5	*qLA8*	73.3-80.0	1.93**	1.35
1stLA	*qLA5.3*	97.9-103.0	*qLA7-1*	15.2-19.3	2.42**	1.96
2ndLA	*qLA3.1*	55.2-59.5	*qLA4-2*	107.8-109.2	-1.90**	2.66
2ndLA	*qLA4.2*	107.8-109.2	*qLA5-3*	88.2-97.2	-2.82**	2.47
2ndLA	*qLA4.2*	107.8-109.2	*qLA7-1*	15.2-19.3	-1.64**	0.6
2ndLA	*qLA5.3*	97.9-103.0	*qLA7-1*	15.2-19.3	2.38**	2.42
2ndLA	*chr9-90756–mmc0051*	47.3-48.1	*chr10-77445–umc1336*	20.6-22.4	-2.05**	2.66
3rdLA	*qLA3.1*	55.2-59.5	*qLA4-2*	107.8-109.2	-1.55**	2.06
3rdLA	*qLA4.2*	107.8-109.2	*qLA5-3*	88.2-97.2	-1.74**	1.38
3rdLA	*qLA5.3*	97.9-103.0	*qLA7-1*	15.2-19.3	1.83**	2.37
3rdLA	*chr9-23536–chr9-32338*	44.7-46.6	*umc1380–chr10-12923*	12.0-13.3	-2.09**	3.04
4thLA	*qLA3.2*	67.9-76.6	*qLA5-3*	81.6-88.2	1.49**	0.69
4thLA	*qLA3.2*	67.9-76.6	*qLA7-1*	15.2-19.3	1.99**	1.61
4thLA	*qLA5.3*	97.9-103.0	*qLA7-1*	15.2-19.3	2.30**	2.57
5thLA	*chr4-150464–bnlg1137*	49.8-65.8	*qLA4-2*	98.4-105.3	1.07*	0.39
5thLA	*chr8-103366–chr8-111393*	39.4-42.6	*chr8-165985–chr8-167777*	84.7-88.3	-2.26**	3.54
6thLA	*qLA4.2*	107.8-109.2	*qLA5-3*	88.2-97.2	-1.06**	1.2
6thLA	*chr8-103366–chr8-111393*	39.4-43.6	*qLA8-1*	72.3-80.0	-2.28*	3.52
7thLA	*qLA2.1*	4.6-14.6	*qLA5-1*	46.3-49.2	1.13*	1.08
7thLA	*phi213984–chr4-10484*	14.6-18.6	*bnlg1759–umc1350*	93.2-94.2	-1.99**	3.25

AA is the additive-by-additive epistatic interaction effect

H^2 (aa)(%) are percentage of variance explained by the additive-by-additive epistatic interaction effect

*, ** and *** Indicate significant level at $P < 0.05$, $P < 0.01$ and $P < 0.001$, respectively

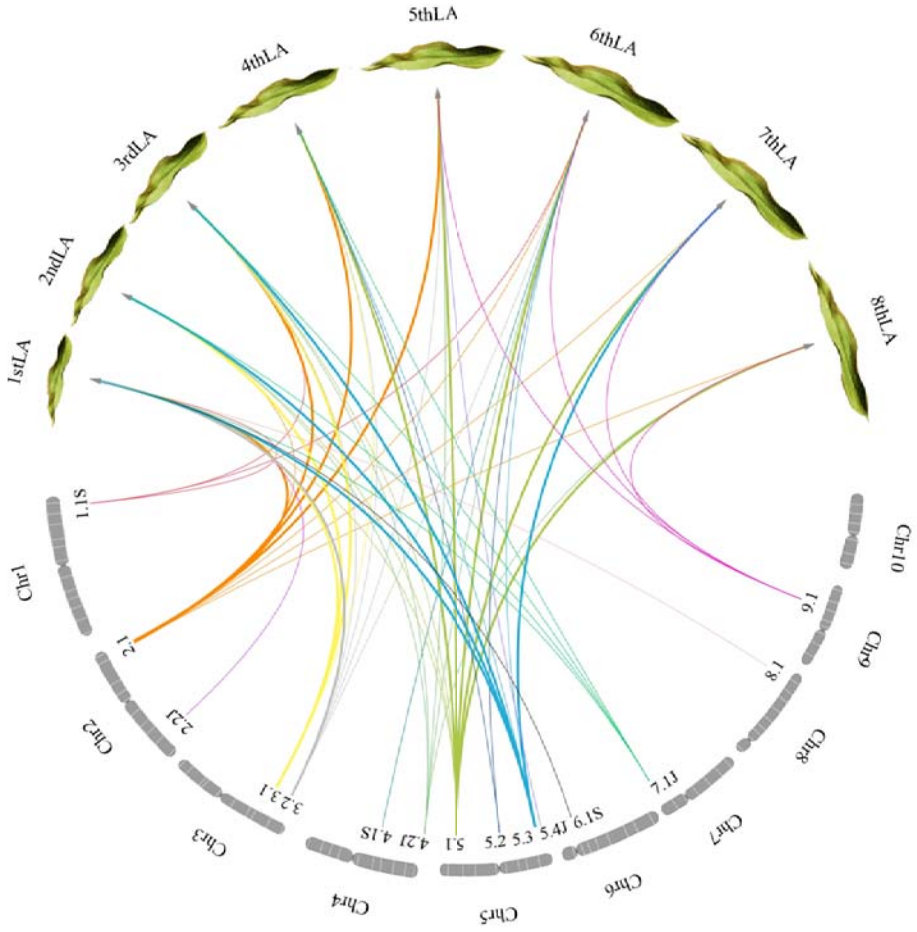

Fig. 1. The network diagram of identified QTL controlled the eight LAs. The 1.1 of Chromosome 1 (Chr1) represents *qLA1.1*, and so forth. The capital letters S and J represent the QTL detected only in single-environment and joint analysis, respectively. The arrowhead lines mean that the QTL control the corresponding LA. Different colored lines represent different QTL. The thick lines represent the PVE (%) of QTL > 10%, fine lines represent the PVE (%) of QTL ≤ 10%. When one QTL was identified in more than one environment or both single-environment and joint analysis, we choose the highest value of PVE.